Electrochimica Acta 512 (2025) 145495

Contents lists available at ScienceDirect

Electrochimica Acta

journal homepage: www.journals.elsevier.com/electrochimica-acta

Assessment of the effect of acids application during the electrodialytic recovery of lithium from mine tailings

Joana Almeida [a,*], Carolina Pires [b], Catarina Branco [a], Eduardo P. Mateus [a], Alexandra.B. Ribeiro [a,*]

[a] CENSE – Center for Environmental and Sustainability Research & CHANGE - Global Change and Sustainability Institute, NOVA School of Science and Technology, NOVA University Lisbon, Campus de Caparica, 2829-516 Caparica, Portugal
[b] Laboratory of Environmental Technology, Department of Chemical Engineering, Federal University of Parana, Curitiba 81530-000, Brazil

ARTICLE INFO

Keywords:
Critical raw material
Lithium
Electro-based technology
Acid
Mine tailings
Decarbonisation

ABSTRACT

Energy transition has been driven by climate change and the need to decarbonize the transport sector. Herein, lithium-ion batteries play a prominent role in transports electrification and renewable energy sources integration, which has been increasing lithium demand worldwide. To alleviate lithium primary resources exploitation, the use of secondary resources of lithium are desirable, considering a circular perspective. Mine tailings are generated in massive volumes, due to low ore grades, and may present contents of lithium-based minerals. Therefore, proper management is required to guarantee the safety of this resource, offering also an opportunity for secondary recovery of critical raw materials, such as lithium. The present work aimed to analyse the potential of the electrodialytic process to recover lithium from mine tailings with lepidolite contents. The addition of inorganic and organic acids was tested, to address the synergy between the electrodialytic process and acids extraction. Pre-heat of the solid suspension and of the solid sample was also considered. Bench scale experiments were conducted considering a two-compartment electrodialytic reactor at 100 mA, with a cation exchange membrane interposed. Eight different acids, at concentrations of 0.1 mol/L and 0.5 mol/L, were tested individually and in mixture, during 3, 4 and 10 days. The highest lithium recovery ratio (29.8%) was obtained for the experiment conducted with oxalic acid at 0.5 mol/L and suspension pre-heated (55 °C) for 24 h These conditions improved chemical reactivity and the dissolution of lithium minerals.

1. Introduction

The transport industry accounts for approximately 25% of global greenhouse gas emissions, turning this sector a top priority for decarbonisation policies [1]. Under the "Fit for 55″ package, the European Union (EU) has set straight targets to decrease net emissions by at least 55% by 2030 (compared to 1990 levels) to achieve climate-neutrality by 2050 [2]. The electric vehicle (EV) market is booming to accomplish net zero emissions, and it is foreseen that EV accounts for about 60% of total vehicle sales in 2030 [3].

Electric vehicles entail the use of batteries with high energy density, which is leveraging technological development in renewable energy and battery storage for innovative power systems with sustainable energy sources [4]. Lithium-ion batteries (LIB), that are made of materials with low toxicity, can be smaller and lighter than the conventional nickel-cadmium batteries, and hold their charge for longer [5].

From the greek *lithos*, that means stone, lithium (Li) is the first metal in the periodic table and the lightest and the least reactive of alkali metals [6]. Globally, minerals and brines represent the main primary source of Li. In 2020, around 22% of global Li production from brine salt flats was from Chile. On the other hand, Australia is the top leader of Li production from pegmatite minerals (e.g. spodumene, lepidolite, petalite and zinnwaldite), accounting for 49% of 2020 global production [7]. Moreover, Portugal has the ninth largest world's amount of Li resources, that is estimated in 60,000 t [8].

Lithium carbonate (Li_2CO_3) and lithium hydroxide (LiOH) are commonly applied during LIB production [9]. Thus, the growing need for high-capacity batteries increased Li extraction from primary resources, where Li demand is expected to increase 14 times in 2040, compared to 2020 levels [10]. Therefore, Li was included on both European Union (EU) lists of critical raw materials (CRM) and strategic raw materials (SRM), due to its current economic relevance, supply risk and

* Corresponding authors.
E-mail addresses: js.almeida@fct.unl.pt (J. Almeida), abr@fct.unl.pt (Alexandra.B. Ribeiro).

https://doi.org/10.1016/j.electacta.2024.145495
Received 30 September 2024; Received in revised form 14 November 2024; Accepted 7 December 2024
Available online 9 December 2024

prominent role in clean energy transition [11].

To empower the research on new pathways that enable Li recovery and reuse towards circular economy principles, the Critical Raw Materials Act established that 25% of the CRM consumption must come from recycled materials [12]. Extensive focus has been directed on Li recovery from obsolete LIB. Despite of technological advances, its contribution to global Li production has remained marginal [13], with global recycling rate for Li being around 5% [14]. Unconventional Li resources, such as rejected fractions from mining activities, industrial waste, and effluents are also being considered, where precipitation, adsorption, ion-exchange, solvent extraction, and membrane electrolysis have been studied [15].

Mining for minerals generates large amounts of byproduct waste materials, composed of ground rocks, lower contents of valuable minerals, chemicals, and processed water [16]. Mine tailings are fine suspended materials frequently stored in the form of slurry in large tailings dams. More than 14 billion t of mine tailings have been produced by the global mining industry only in 2010. Currently, the ore grades decrease tendency will promote a massive volume of future tailings that needs to be properly managed [17].

Lithium recycling from mine tailings with Li contents could reduce the supply demand of primary raw materials, alleviate the domestic Li supply chain and economic condition and the environmental impacts related to mine tailings production and storage [18].

Furthermore, the application of electro-based technologies has shown promising results in the recovery of CRM and SRM from secondary solid sources, such as phosphorus (P) from sewage sludge [19], tungsten (W) from secondary mining resources [20], copper (Cu) from treated timber waste [21] and light rare earth from soils [22]. In particular, the electrodialytic (ED) process promotes the removal and/or recovery of substances from an environmental sample, based on the application of a low-level current density (mA/cm^2) between a pair of electrodes placed in an ED reactor divided with ion exchange membranes [23]. Chemical species are mobilized through the transport mechanisms that occur (e.g., electrodialysis, electroosmosis, electromigration, electrophoresis, diffusion) and ion exchange membranes are used to separate the matrices and increase the selectivity of the CRM to be recovered [23]. To optimize the effectiveness of the ED process for metal extraction from matrices, the application of assisting agents, such as extracting solutions or solvents, has been documented [24].

The present research work explores the efficiency of the ED process on the recovery of Li^+ from mine tailings, with the aid of organic and inorganic acids. The experimental tests were carried out at bench scale, using a two compartment ED reactor and a cation exchange membrane (CEM).

2. Materials and methods

2.1. Sample initial characterisation

The mine tailings (MT) sample used for the present research is pegmatite based, and contains lithified feldspars with Li. The sample was collected at 12 m depth of a mine tailings deposit in Portugal and is characterised by a particle size of 2 mm. The company that provided the MT sample supplies the ceramic industry through feldspar with Li, as primary activity.

For the MT initial characterization, the Li content was addressed, as well as pH and conductivity in a water suspension with a liquid-to-solid ratio (L:S) of 40.

Lithium concentrations were determined by Inductively Coupled Plasma with Optical Emission Spectrometry (ICP-OES) (HORIBA Jobin-Yvon Ultima, Japan), at Chemical Analysis Laboratory from REQUIMTE/LAQV (NOVA University Lisbon, NOVA School of Science and Technology, Portugal). The pH and conductivity were measured with an EDGE electrode meter (HANNA Instruments, Rhode Island, USA).

The MT total quantitative chemical analysis was conducted by X-ray fluorescence (XRF) spectrometry, in a PANalytical Axios Max spectometer (Malvern, United Kingdom). As a complement, the SciAps Z-903 portable Laser Induced Breakdown Spectroscopy (LIBS) instrument (Massachusetts, USA) was used to analyse the MT. The SciAps GeoChem App was selected to provide a quantitative measurement of each element present in the sample, through factory-built calibrations, between ppm and %.

2.2. Lithium desorption

2.2.1. Preliminary desorption tests

The optimal pH to desorb the Li content from MT was studied through desorption tests: 1 g of mining residues were suspended in 20 mL of different concentrations of HNO_3 and NaOH, as well as in deionized H_2O, to generate solutions with pH between 2 and 8, for 24 h

In addition, the Li desorption behaviour was analysed in the presence of organic acids, such as citric acid (CA) and oxalic acid (OA), considering concentrations between 0.5 mol/ L and 2.0 mol/L.

2.2.2. Final desorption tests

As OA demonstrated the highest Li desorption, MT were suspended in a solution with OA concentrations between 0.5 mol/L and 1.5 mol/L, for 24 h, 48 h, 72 h, and 96 h

For desorption tests, all the suspensions were placed in a shaking table at 200 rpm, at room temperature (approx. 20 °C). At the end, pH was measured with an EDGE electrode meter (HANNA Instruments, Rhode Island, USA). The suspensions were filtered by vacuum using MFV3 glass microfibre filters (pore size = 1.2 μm and diameter = 47 mm; Filter Lab, Barcelona, Spain), and Li concentrations were determined by ICP-OES.

2.3. Electrodialytic experiments

The bench scale experiments were carried out in two-compartment (2C) ED acryl XT reactors (RIAS A/S, Roskilde, Denmark). The sample was placed in the anode end, and the electrolyte solution in the cathode compartment. Both compartments have an internal diameter of 8 cm, a length of 10 cm in the sample compartment, and a length of 5 cm in the cathode compartment. The CEM used was from Ionics (CR67, MKIII, Blank, USA). A pair of electrodes made of titanium/MMO (metal mixed oxides) Permaskand wire, with a diameter of 3 mm and a length of 50 mm (Grønvold & Karnov A/S, Denmark) were introduced in each compartment. A power supply (Hewlett Packard E3612A, USA) maintained a constant direct current of 100 mA. A stirrer (Heidolph, Germany; VELP Scientifica Srl, Italy) was placed into the sample compartment, at 200 rpm, to prevent the sample from settling during the experiments. Fig. 1 depicts the configuration of the 2C ED reactor.

For all experiments, 250 mL of sodium nitrate ($NaNO_3$), at a concentration of 0.02 mol/L, was introduced as catholyte in the cathode compartment. The sample suspensions were prepared with deionized water, MT, and acids at different concentrations, as listed in Table 1. A pre-heat of the sample suspension in a hot plate digital stirrer RSLab-2C for 24 h at 55 °C was tested. Also, the solid sample pre-heated in a muffle furnace (Nabertherm, Lilienthal, Germany) at 800 °C for 1 h was considered for the experiments.

The experiments were operated for 3, 4, and 10 days, and it was also tested 1 day pre-heat at 55 °C, followed by 3 days of ED process. The ED reactors were placed inside a fume hood (Industrial Laborum Ibérica, Portugal), at room temperature (circa 20 °C). Throughout the experimental period, the voltage of each reactor was registered, and pH and conductivity of both the catholyte and sample compartments were daily monitored. Samples were collected from the reactor and analysed with HANNA EDGE pH and conductivity meters, and then returned to the ED reactor.

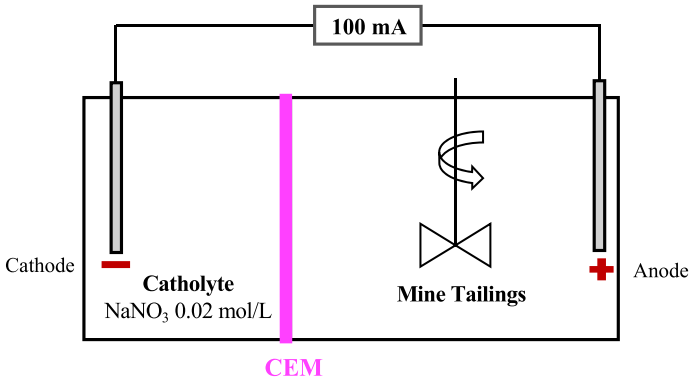

Fig. 1. Electrodialytic reactor configuration applied during the bench scale experiments (CEM - Cation Exchange Membrane).

Table 1
Operation time, pre-heat conditions and acids tested during electrodialytic experiments.

Duration / pre-heat	Acid	L:S	Experiments code
3 days	Malonic Acid 0.1 mol/L	9	MA3dL9
	Formic Acid 0.1 mol/L	9	FA3dL9
	Acetic Acid 0.1 mol/L	9	AA3dL9
	Citric Acid 0.1 mol/L	9	CA3dL9
	Oxalic Acid 0.1 mol/L	9	OA3dL9
	Citric Acid 0.1 mol/L	40	CA3d
	Oxalic Acid 0.1 mol/L	40	OA3d
4 days	Oxalic Acid 0.5 mol/L	40	OA4d
	Oxalic Acid + Nitric Acid 0.5 mol/L	40	OA+NA4d
	Oxalic Acid + Sulfuric Acid 0.5 mol/L	40	OA+SA4d
	Sulfuric Acid 0.5 mol/L	40	SA4d
	Gluconic Acid 0.1 mol/L	40	GA4d
1 + 3 days Pre-heating suspension = 55 °C	Oxalic Acid 0.5 mol/L	40	OA1+3dh
1 + 3 days Pre-heating suspension = 55 °C + stirring	Oxalic Acid 0.5 mol/L	40	OA1+3dhs
3 days Pre-heating solid phase = 800 °C	Citric Acid 0.1 mol/L	40	CA3dh
10 days	Oxalic Acid 0.5 mol/L	40	OA10d

2.4. Lithium determination

At the end of each experiment, the ED reactor was disassembled, and both electrodes and membranes were immersed in HNO_3, 5 mol/L and 1 mol/L, respectively, for 48 h, to ensure the removal of Li^+. The electrodes and membrane were stored in glass containers sealed with Parafilm M (Neenah, Wisconsin), to prevent evaporation. After this period, the volumes of acid used were measured for each electrode and membrane, and samples were collected for ICP-OES analysis.

To separate solid and liquid phases from the sample compartment, a vacuum filtration was conducted using a lab vacuum pump (KNF LABOPORT, Freiburg, Germany), connected to a 500 mL vacuum filtration flask (DURAN, West Germany). The solution passes through with a filter paper (pore size = 11 μm and diameter = 150 mm; Whatman, United Kingdom) placed on a Buchner funnel. The process was performed within a portable fume hood (FUMEX MEB 1300–75, Västerbotten, Sweden). The liquid phase was stored in a fresh and dry place, at room temperature (approx. 20 °C) until ICP-OES analysis.

On the other hand, the final solid phase was collected, left to dry in the fume hood for a week, and subsequently submitted to microwave-assisted digestion on a Milestone Ethos Microwave Digestion/Extraction System (Bergamo, Italy).

The EPA3051A [25] microwave (MW) extraction method was followed, by adding to the digestion vessels 0.5 g of dry sample, 9 mL of HNO_3 and 3 mL of HCl, in a fume hood.

Following the MW-assisted extraction program and the vessels cool down, the samples were submitted to vacuum filtration, using MFV5 glass microfiber filters (pore size = 0.7 μm and diameter = 47 mm; Filter Lab, Barcelona, Spain). Subsequently, the samples were diluted to 25 mL with deionized water, to be further analysed by ICP-OES. The ICP-OES analysis yielded results for Li content measured in mg/L across the various components of the ED reactor. To determine the ED process recovery efficiency for Li^+, Eq.1 was applied:

$$Li^+ \ recovery \ (\%) = \frac{Li^+{}_{catholyte \ (mg)} + Li^+{}_{Liquid \ phase \ (mg)}}{Total \ Li^+ \ (mg)} \quad \text{(Eq. 1)}$$

2.5. Reagents and standards

For the bench scale tests, the reagents and standards applied are summarized in Table 2.

3. Results and discussion

3.1. Initial characterisation

To assess the influence of the media conditions during the recovery processes, measurements of pH, conductivity and Li content were conducted on the initial sample. The Li content was determined using ICP-OES. Table 3 presents the initial characterization, where pH and conductivity were measured in a L:S of 40, in deionized water. Four measurements were conducted ($n = 4$).

The initial conductivity of MT was 0.015 mS/cm, which is extremely low to ensure the current passage during the ED process without the addition of enhancing agents. The pH exhibited a value of 6.6. Regarding the target compound, the analysis revealed that Li amount is 1274.8 ± 210.6 mg/kg. Table 4 presents the chemical composition of MT performed by XRF. The main species detected is SiO_2 (67.18%), communally called silica and the most abundant compound on Earth [26], followed by Al_2O_3 (19.95%), aluminium oxide. Lepidolite ($KLi_2Al(Al,\ Si)_3O_{10}(F, OH)_2$), that is the main mineral present in the MT study sample and contains significant amounts of aluminium [27].

In practice, for the XRF spectroscopy, the detection of elements lighter than titanium (Ti), Z = 22, has been challenging. The difficulty ascends due to the low fluorescence yield from these elements, and the attenuation of this yield by the detector window and the air atmosphere. On the other hand, LIBS is inherently more sensitive and better suited for light element detection [28]. Table 5 presents the LIBS analysis of the MT, as a complement of XRF characterisation.

The results achieved for Li contents using LIBS (437 ± 186 mg/kg)

Table 2
Reagents and standard used for the experimental tests.

Reagent/ Standard	Purity (%)	CAS	Brand	Origin
Nitric acid, HNO_3	≥65%	7697–37–2	Honeywell Fluka	Charlotte, USA
Sodium hydroxide, NaOH	≥98%	1310–73–2	Merck	Darmstadt, Germany
Deionized H_2O	–	–	Water purification system from Thermo Fisher Scientific	Waltham, USA
Citric acid, CA	99%	5949–29–1	Merck	Darmstadt, Germany
Oxalic acid, OA	99.5–102.0%	6153–56–6	PanReac AppliChem ITW Reagents	Monza, Italy
Sodium nitrate, $NaNO_3$	≥99%	7631–99–4	PanReac AppliChem ITW Reagents	Monza, Italy
Malonic acid, MA	99%	141–82–2	Thermo Scientific Chemicals	Waltham, USA
Formic acid, FA	99%	64–18–6	Carlo Erba Reagents	Milan, Italy
Acetic acid, AA	≥99.8%	64–19–7	Honeywell Fluka	Charlotte, USA
Sulfuric acid, H_2SO_4	95–97%	7664–93–9	Merck	Darmstadt, Germany
Gluconic acid, GA	49–53 wt.% in H_2O	526–95–4	Merck	Darmstadt, Germany
Hydrogen chloride, HCl	37%	7647–01–0	PanReac AppliChem ITW Reagents	Monza, Italy

Table 3
Initial characterisation of the mine tailings sample ($n = 4$).

Mine tailings		
Li (mg/kg)	pH	Conductivity (mS/cm)
1274.8 ± 210.6	6.6 ± 0.4	0.015 ± 0.032

and ICP-OES (1274.8 ± 210.6 mg/kg) diverge. LIBS is less sensitive than ICP-OES, once ICP-OES excitation is continuous compared with the low frequency of the laser ablation (10 Hz) from LIBS. Furthermore, the sample preparation for ICP-OES analysis promotes the total digestion and homogenisation of the sample (by MW-assisted extraction), while LIBS analysis is punctual and superficial, being affected by the heterogeneity of the sample [29].

Based on the chemical analysis, certain elements in the MT may form compounds with Li, during the ED process. The application of organic and inorganic acids can also lead to the formation of Li complexes. From Tables 4 and 5, the following metallic elements are in MT: Ca, K, Mg, Al, Na and Ti. Due to the repulsive nature of cations, it is not expected that these elements form stable compounds with Li [30].

3.2. Desorption tests

The comprehension of metal-soil interaction allows to predict how changes in environmental conditions (e.g. pH) could affect metals mobility [31]. Chemical desorption includes the desorption of an attached molecule/substance from a solid surface [32]. For the removal of the metal ions from the matrix's surfaces, several desorbing agents can be applied, such as acids, alkalis, salts and chelating agents [33].

The optimal pH to solubilise the Li content from MT was studied through desorption tests, that were conducted with organic and inorganic acids. Fig. 2 presents Li desorption in solutions with pH between 2 and 8, for 24 h, at different concentrations of HNO_3 and NaOH solutions. Herein, is visible that the desorption process starts at pH<4 with the experimental highest Li desorption occurring at the lowest studied pH, 2.

In addition, Li desorption behaviour was also analysed in the presence of organic acids, such as CA and OA, as shown in Fig. 3. The OA demonstrated a higher potential to solubilize Li, once higher desorption was observed at all concentrations of acids tested. Oxalic acid is a strong organic acid that can dissolve metal ions from minerals by breaking down the crystal lattice of Li-bearing compounds, such, lepidolite. The acid donates protons (H^+), which facilitate the breaking of bonds in these minerals, allowing Li^+ to be released [34].

The OA is a diprotic acid, where $pKa_1 = 1.46$ and $pKa_2 = 4.40$ [35]. On the other hand, CA is a triprotic acid, with $pKa_1 = 2.79$; $pKa_2 = 4.38$ and $pKa_3 = 5.68$ [36]. The pKa may be allied to the initial/final pH observed, meaning that pH(OA) < pH(CA). Based on Fig. 3, if Li solubilization is related to pH fluctuation, it is foreseen that Li desorption by OA will be higher than in the presence of CA. Additionally, the pH in solution of CA at 0.1 mol/L is 2.08. In the case of OA, for the same concentration, 0.1 mol/L, it exhibits a value of 1.31 [37]. The Li^+ concentration is related to the concentration of the acids, pH and time, being the pH a function of the acid's concentration. Once the pH of the OA solution is lower than CA, the concentration of $Li^+$is higher.

Bearing in mind that OA demonstrated the highest Li solubilisation, the MT sample was suspended in a solution with OA concentrations between 0.5 mol/L and 1.5 mol/L, for 24 h, 48 h, 72 h and 96 h (Fig. 4). The highest solubilization of Li was observed when 96 h of operation time was tested. At 24 h and 48 h, a drop after 1.0 mol/L was observed. The properties of the bidentate oxalate ion may have contributed to form oxalate complexes with Li, forming precipitates and decreasing the concentration in the liquid phase of the suspension, since OA may react with other solubilized elements [38].

3.3. ED experiments

Electrodialytic experiments were performed considering the addition of different acids to assess the Li^+ recovery potential from MT. A 2C reactor was applied (Fig. 1), once direct acidification of the sample suspension through half-reactions at the anode ($H_2O \rightarrow 1/2O_2 + 2H^+ + 2e^-$) decreases pH and increases the mobilization of species. Therefore,

Table 5
Analysis of each element present in the sample by Laser Induced Breakdown Spectroscopy.

mg/kg								
Si	Al	Fe	C	Ti	Li	Ba	Mn	Be
459,100 ± 24,800	91,000 ± 8480	5144 ± 1051	2734 ± 758	809 ± 130	437 ± 186	169 ± 23	89 ± 32	9.8 ± 2.4

Table 4
Total quantitative chemical analysis of mine tailings sample by X-ray fluorescence spectrometry.

Percentage (%)										
SiO_2	Al_2O_3	Fe_2O_3	CaO	MgO	K_2O	Na_2O	TiO_2	MnO	P_2O_5	L.I.*
67.18	19.95	0.81	0.07	0.25	3.35	3.06	0.12	0.05	0.22	4.48

* L.I. – Loss on ignition.

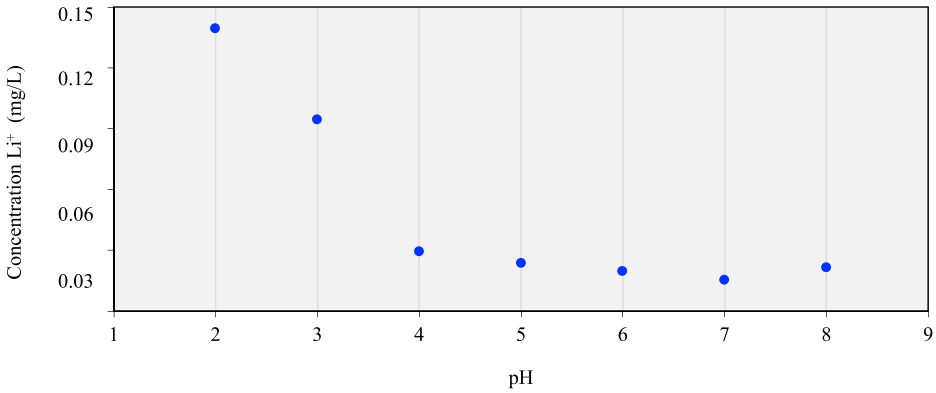

Fig. 2. Lithium desorption tests at different concentrations of HNO_3 and NaOH solutions with pH between 2 and 8.

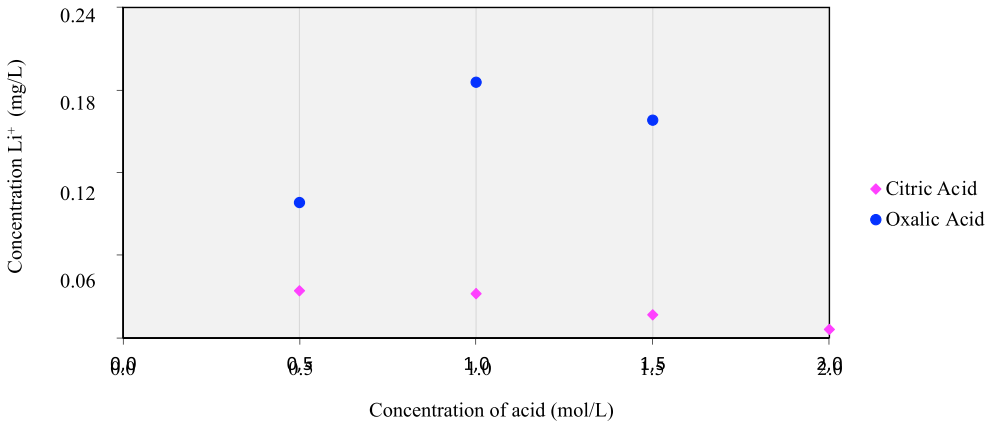

Fig. 3. Lithium desorption tests at different concentrations of organic acids.

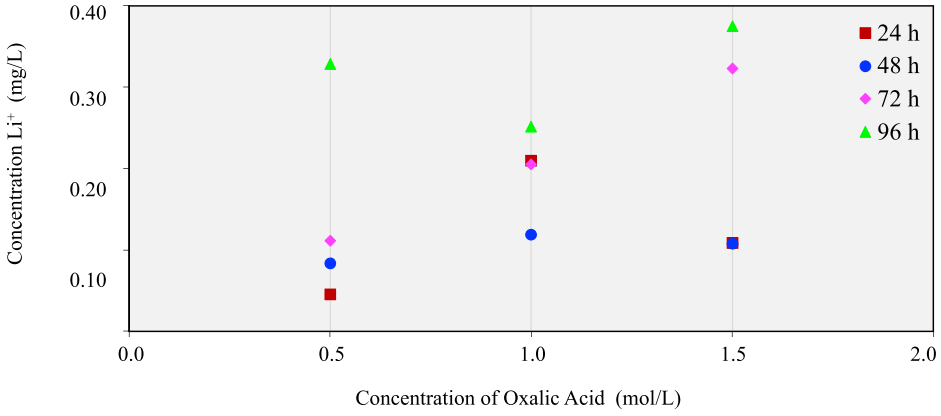

Fig. 4. Lithium desorption tests at different concentrations of oxalic acid and operation times.

for most metals, this also results in higher removal from the sample suspension [39]. In addition, as observed in desorption tests (Section 3.2), the Li dissolution in an acidic media is higher than in an alkaline media.

3.3.1. pH

The pH evolution in both sample and catholyte compartments is presented in Fig. 5. It is possible to perceive a relation between the acids pKa and the initial pH in the sample compartment. Therefore, three groups are observed: group I with pH $>$ 3 (only includes CA); group II with pH between 2 and 3 and; group III with pH $<$ 2. Grouping by pH can reveal differences in chemical behaviour, stability, solubility, or reaction rates associated with the acidity of the environment. Group I represents a particular case, when CA was applied, demonstrating unique characteristics at higher pH levels.

In the anode (sample compartment), while generally stable, pH exhibits a rise for almost all the experiments. Despite the expectation of a decrease of pH in the sample compartment, owing to the formation of H^+due to water electrolysis at the inert anode, the transport of the acid front is retarded by the buffering capacity in this compartment. Cation exchange capacity of the minerals, and availability of organic species and salts may react with the acid and increase the buffering capacity

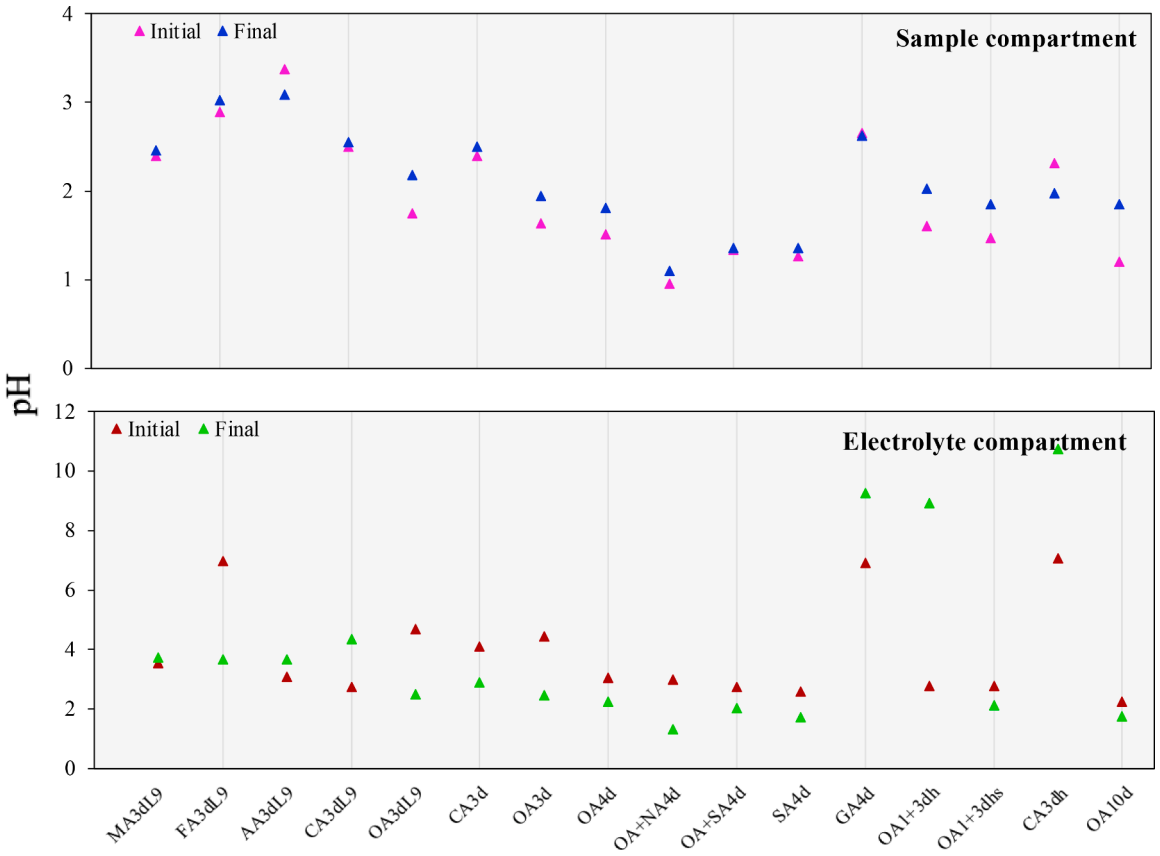

Fig. 5. pH variation during the electrodialytic experiments.

[40]. Additionally, the electromigration of H^+ through the CEM into the cathode compartment, and electrochemical reactions that involve the consumption of H^+ ions may explain the final pH increase. At the end of the ED process, the pH in the MT compartment oscillated between 1.10 (OA + HNO_3) and 3.09 (AA).

In the electrolyte compartment (catholyte), it would be expected to observe an overall increase of pH due to OH^- ions formed due to the water electrolysis in the cathode. However, once acids at different

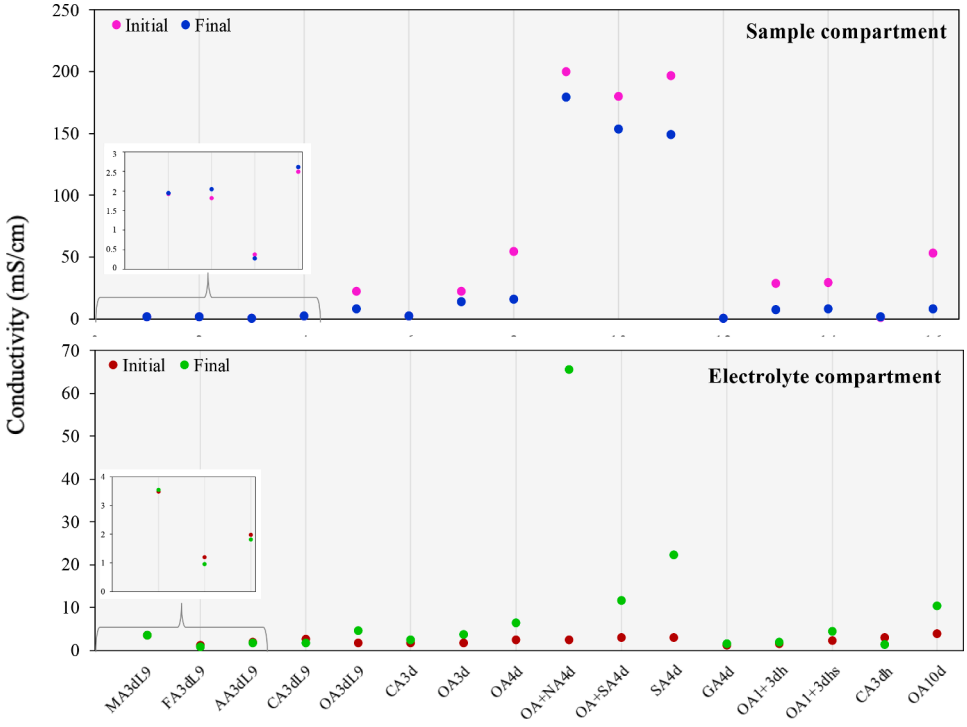

Fig. 6. Conductivity variation during the electrodialytic experiments.

concentrations were added, a constant acidification of the media was observed in the experiments conducted with stronger acids, as observed for the cases that involved FA (FA3dL9), OA (OA3dL9; OA3d; OA4d; OA1+3dhs; OA10d), CA (CA3d), H_2SO_4 (SA4d) and H_2SO_4 with OA (OA+SA4d), and OA with HNO_3 (OA+NA4d). The acid dissociation constant, pKa, from OA is 1.46, and is more acid than the other organic acids [35]. The strongest acids are the inorganic ones: H_2SO_4 (pka = −3; 1.99) and HNO_3 (pka = −1.3) [41]. A lower pKa indicates greater tendency to donate protons and to form soluble metal complexes, thus facilitating the release of metal cations into the solution [41], which may explain the behaviours observed in Fig. 5. The solubility of oxides, hydroxides, carbonates or mineral forms depends on the suspension pH [42].

3.3.2. Conductivity

The conductivity variation along the ED experiments is depicted in Fig. 6. In the electrolyte compartment (catholyte) a steady increase over time was observed. It is noticeable that the conductivity of MT increased in comparison to the initial characterization of the sample (Table 3). Conductivity in the media must be assured to promote current passage and electro-chemically induced extraction of substances [20]. The conductance is the reciprocal of the Ohm, the unit of resistance. As conductivity and conductance are positively correlated, elevated conductivity levels result in decreased resistance [43].

In the sample compartment, all tests exhibited a decline in their conductivity levels over time, suggesting that electromigration from the anode compartment through CEM towards the cathode occurred. The higher conductivity in the electrolyte was observed with OA + HNO_3 (65.53 mS/cm) and H_2SO_4 (22.31 mS/cm), that are the most acidic reagents used.

3.3.3. Voltage

Fig. 7 presents the voltage registered in the ED reactor. Generally, the voltage decreased after the experiments. As ohmic resistance increases, so does the voltage drop. The increase in resistance could be attributed to the dissolved metal amount or to the formation of neutral charged molecules. The effects of different solute metals may vary over a considerable range. Resistance may be caused by thermal motion of the atoms, impurities, or disorder existing in a liquid [44].

The opposite trend was verified for the voltage in FA3dL9, GA4d, OA1+3dhs, CA3dh and OA10d. The higher voltage at the end can be attributed to the declining conductivity observed in the anolyte over time (Fig. 6). The voltage increased means a decrease in the resistivity, according to Ohm's Law [45]. Additionally, the fluctuating voltage levels could be attributed to the utilization of different enhancements and operation times [46]. Such variability highlights the strong dependence of voltage evolution with the type of enhancement used and experiment duration, and its influence on the process performance.

3.3.4. Lithium recovery

As presented in Table 1, acids were tested to address Li^+ extraction efficiency from MT. Table 6 presents the Li^+ recovery of the different ED configurations. The highest yield was obtained when OA (organic acid) and H_2SO_4 (inorganic acid) were tested, with a recovery efficiency of approximately 30%. It was expected that as the pH in the MT suspension decreases the dissolution of Li increases. In fact, an acidic sample media was observed when OA (pH = 2.03) and H_2SO_4 (pH = 1.36), at 0.5 mol/L, were applied (Fig. 5), which corroborates a higher Li dissolution at a lower pH.

The results also indicate the influence of the operation time and temperature on the pre-treatment of the sample, once on OA1+3dh, a pre-heat for 24 h of the suspension was performed, followed by the 3 days of ED treatment. With this configuration, the recovery of Li^+achieved 29.82%. While both methods may yield similar Li recovery rates, the ED process coupling OA offers potential benefits in comparison

Table 6
Electrodialytic extraction yield of lithium from MT, and amount of lithium that remained in the solid phase, at the end of the experiments.

Experiment	Li^+ recovery		Li in the solid phase (%)
	%	mg/kg	
MA3dL9	3.04	3.34	96.96
FA3dL9	2.07	2.27	97.93
AA3dL9	2.8	3.07	97.20
CA3dL9	4.42	4.85	95.58
OA3dL9	6.96	7.64	93.04
CA3d	4.03	4.43	95.97
OA3d	8.14	8.92	91.86
OA4d	21.79	23.92	78.21
OA+NA4d	25.45	27.94	74.55
OA+SA4d	12.07	13.24	87.93
SA4d	29.26	32.12	70.74
GA4d	2.25	5.64	97.75
OA1+3dh	29.82	32.73	70.18
OA1+3dhs	24.81	27.23	75.19
CA3dh	17.19	18.98	82.81
OA10d	11.90	13.06	88.10

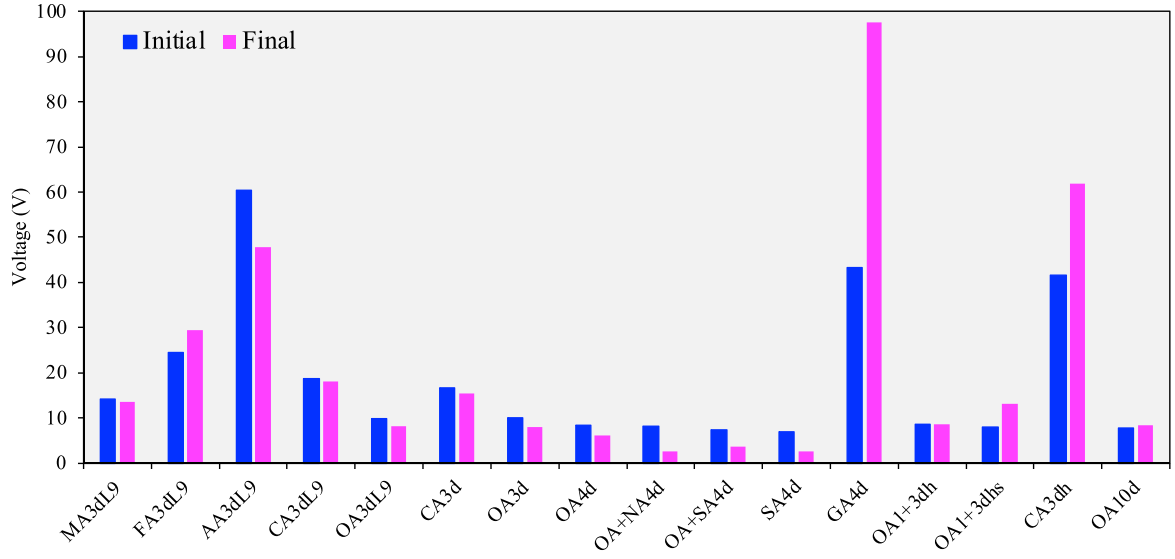

Fig. 7. Voltage variation during the electrodialytic experiments.

to H_2SO_4 applications, particularly in terms of environmental sustainability, safety, and operational efficiency. The ability to selectively separate Li^+, the reduced chemical usage, and lower environmental impact turn the ED process an attractive choice. H_2SO_4 is a strong, corrosive substance that can cause harm to the environment if not handled properly. The waste generated from acid leaching often contains toxic residues and must be neutralized before disposal, leading to additional treatment steps. On the other hand, the ED process coupling OA primarily uses electrical energy to drive the selective ion exchange through ion-exchange membranes, not involving harmful chemicals. Moreover, it typically generates fewer hazardous waste products compared to acid leaching. Oxalic acid and its complexes are biodegraded in aerobic and anaerobic conditions in soil and water in less than one day [47], turning the application of OA more attractive than the conventional inorganic strong acid.

Heat treatment is commonly applied to enhance the chemical reactivity of MT, as this treatment can favour chemical reactivity, depending on the mineralogy of the tailings and the use of an optimal temperature. The combination of thermal treatment in the acid environment may enhance the dissolution of minerals [48].

However, Li^+ recovery process may depend on other variables, such as pH, leaching agents, solid-liquid ratio, or reaction time. Heat treatment might not have shown significant benefits if these other factors are not optimized, so further developments could evaluate the preheating process together with a full set of experimental parameters.

Although stirring during the pre-heat of the sample suspension at 55 °C was tested for the same setup (OA1+3dhs), no improvements were observed in the Li^+ recovery. The amount of Li^+ recovered from MT was 24.81%. Stirring leaching includes the dispersion of finely ground ore into an acid solution. This mixing process avoids particle precipitation and promotes leaching kinetics [49]. During the ED process, stirring was important to facilitate the diffusion of Li^+ from the solid sample into the liquid phase.

Additionally, a higher L:S promoted higher Li solubilization and recovery yields. At L:S of 9, the Li^+ recovery oscillated between 2.07% (FA3dL9) and 6.96% (OA3dL9), while at L:S of 40 achieved 29.82%. This ratio also plays an important role in the kinetics, because it is related to the dissolution and diffusion of metal ions, as well as the mixing conditions in slurry-phase systems [50].

Half of the ED experiments conducted presented Li^+ recovery yields above 10% (Table 6). When acids are employed as assisting agents, it is anticipated that a low pH will promote the liberation of metal cations from the sample, alongside the formation of salts and potential acid–metal complexes, depending on the type of acid applied [46]. However, some minerals are generally difficult to leach without a reductant. Metals can be present in sulphide or oxide minerals in a state with low solubility in aqueous solutions, resulting in a low rate of leaching of these minerals [49].

In general, minerals that contain Li have a crystalline structure composed of tetrahedral chains of silicon and octahedral parts of aluminium linked to Li^+. These structures have high chemical stability due to the mineral's covalent bonds, turning the process of extracting the constituents of the crystalline arrangement difficult [51].

The Li^+ recovery could have been affected by the MT particle size. The specific surface area of a particle depends on porosity, shape, pore size distribution, roughness and size, and commonly shows a stronger correlation with the dissolution rate of the element [52]. The agglomeration of powdered particles could have occurred, affecting the extraction of Li. This can also be linked to the morphological characterization of the MT. If there is no such particle interaction, a significant size reduction and mineral liberation would be predicted [48]. According to Zhang et al. (2021), a particle size of 74 μm could enhance Li extraction from MT, as both larger and smaller particle sizes reduced the leaching rate [53]. However, the particle size of MT in this work was 2 mm (2000 μm), which could also have affected the ED Li^+ recoveries observed. Fig. 8 shows the distribution of the total Li content extracted from the solid sample placed in the anode compartment, that was found in the catholyte solution, and its content in the liquid phase of the anode compartment.

In the OA1+3dh, the experiment that demonstrated higher Li^+ recovery, 50% of the total Li solubilised electromigrated to the catholyte, with approximately 42% remaining in the liquid phase (anolyte) of the anode compartment. Contrary, in SA4d, where the second highest Li^+ recovery was observed, 91% of the Li was found in the sample compartment (anolyte), and only 8% electromigrated towards the catholyte. Generally, with the addition of inorganic acids to ED experiments, the Li solubilized that remained in the sample compartment (anolyte) was between 86% and 94%. Thus, inorganic acids did not facilitate the electromigration of the $Li^+$to the catholyte. Formic and acetic acids, organic acids with the lowest molecular size, have demonstrated the higheost content of Li solubilized in the catholyte, where 85% and 86% of the total Li extracted from the MT, respectively, electromigrated to the cathode compartment. The Li^+ that successfully electromigrated during the ED experiments can be further separated and applied during fabrication of cathodes for rechargeable batteries.

A CEM interposed between the cathode compartment and the sample suspension prevented the passage of negatively charged ions into the sample and will allow the cations, as Li^+, to pass from the sample suspension into the cathode compartment, increasing the selectivity of the final solutions [54].

The solubility of Li is key factor for the Li^+ recovery. The increased solubility of the targeted elements transforms them into mobile ionic species capable of electromigrating towards the cathode compartment. The presence of various elements within MT, coupled with the use of the acids, can lead to the formation of Li salts and complexes in the anode compartment. Salts containing Li^+, Na^+ and K^+, that are present in MT (Tables 4 and 5) are soluble to very soluble in deionized water. Lithium oxide (Li_2O) is not soluble or insoluble in water and reacts readily with water forming LiOH [55], and with carbonate ions to form Li_2CO_3 [56].

In the pH range of 5 to 9, oxalate ion is predominant. Lithium can react with oxalate ($C_2O_4^{2-}$) and form Li oxalate ($Li_2C_2O_4$). The excess OA can react with $Li_2C_2O_4$, forming Li hydrogen oxalate ($LiHC_2O_4$) [57]. In the ED experiments, MA may act as a reductant by donating electrons to Li^+. A potential reaction involving MA may lead to the formation of Li malonate ($Li_2C_3H_2O_4$) [58].

Ion exchange membranes should have a high selectivity in the transport of specific ionic species, while retaining other charged and/or uncharged components [59]. In the ED Li extraction from MT, Li may have remained dissolved in the anolyte as neutral or negatively charged compounds. MT complexes formation may have avoided Li^+ from migrating to the catholyte.

The high presence of Si (67.18%) in the MT can cause significant blocking within the ED reactor and can affect ion-exchange membranes performance [60]. Moreover, lepidolite contains significant amounts of aluminium, that is complex to be removed due to the various forms of ions: Al^{3+}, AlO^{2-}, $Al(OH)_3$, $Al(OH)_2^+$, $Al(OH)^{2+}$ in the aqueous phase [27].

The recovery of minerals occurring in the least concentration can frequently face limitations because of the presence of other metals found in higher concentrations within MT. It is not only base metals that affect the recovery of critical minerals, but various undesirable competing ions such as Ca^{2+}, Mg^{2+}, Zn^{2+}, Fe^{2+}, Fe^{3+} and Al^{3+}can hinder separation processes for critical minerals. In particular, the presence of Fe, Al, and Ca, can significantly impact the dissolution of Li in MT, interfering by consuming OA, competing with Li for complex formation, or forming insoluble precipitates that reduce Li recovery efficiency. To achieve high extraction rates of the target minerals these impurities need to be prior separated from the MT [61]. The removal of aluminium from solutions often needs the addition of acid, base, or extractant, which could also affect a subsequent Li^+ recovery. The Li^+ is characterised by a small radius, presenting a high hydration level, which promotes the increase of the molecule size and a decrease in its mobility [27].

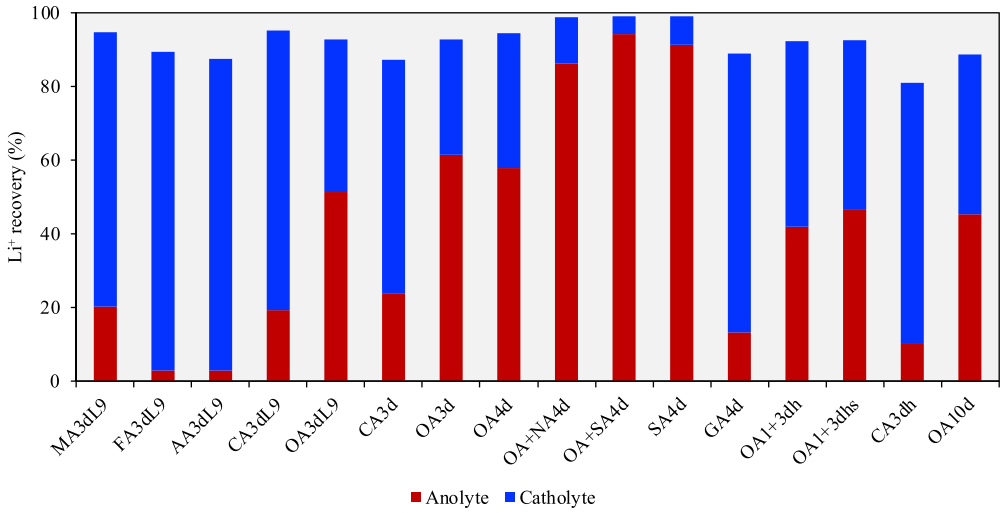

Fig. 8. Lithium recovery in the anolyte and in the catholyte, at the end of the electrodialytic experiments (normalised).

4. Conclusions

Novel and innovative sustainable routes that promote added value to secondary resources are attracting attention in several fields. In particular, the recovery of Li from mine tailings can alleviate negative impacts of primary Li production, the dependency on EU imports of raw materials and the environmental pressures related to massive mine tailing's production and storage. Feasible alternatives that allow Li to be incorporated into the economy in a circular pathway is now key factor to turn energy transition socially and environmentally equitable.

The application of the electrodialytic process coupling OA, that undergoes biodegradation in water within a day or less, promoted a Li^+ recovery of 29.82%. These findings demonstrated a potential new way to recycle Li from mine tailings, reducing environmental risks and providing a secondary source of Li. While its recovery rate is lower than traditional methods like acid leaching, it has advantages in terms of lower environmental impact, reduced energy consumption, and potential cost savings. When compared to other recovery methods, it may offer a good balance of efficiency and sustainability, namely in contexts where mine tailings are abundant, but primary extraction methods are either too costly or environmentally damaging.

When H_2SO_4 was tested, 29.26% of Li^+ was recovered from the original sample. However, in the presence of oxalic acid, 50% of the total solubilized Li electromigrated towards the catholyte, with approximately 42% remaining in the liquid phase of the anode end. Contrary, with H_2SO_4, 91% of the Li^+ was found in the sample compartment (anolyte), and only 8% electromigrated towards the catholyte. The results obtained demonstrate that the oxalic acid proved to be more efficient in facilitating the migration of Li^+ from the anolyte to the catholyte.

The nature of the sample strongly affected the performance of the ED process. Minerals are structure stable matrices, turning Li recovery more complex. Some constrains to ED Li^+ recovery could be attributed to the formation of Li compounds, the high presence of Si, the particle size, and overall low conductivity of MT.

Finally, as Li^+ moves across the CEM, it reacts with OH^- in catholyte to form LiOH, from where it can be recovered. This compound is mainly used for the fabrication of cathodes for rechargeable batteries. By enhancing Li recovery capabilities, EU can improve competitiveness in the value chain of battery storage.

CRediT authorship contribution statement

Joana Almeida: Writing – review & editing, Writing – original draft, Methodology, Data curation, Conceptualization. **Carolina Pires:** Writing – review & editing, Methodology, Data curation. **Catarina Branco:** Writing – review & editing, Data curation. **Eduardo P. Mateus:** Writing – review & editing, Validation, Resources, Formal analysis. **Alexandra.B. Ribeiro:** Writing – review & editing, Validation, Supervision, Resources, Project administration, Funding acquisition, Formal analysis.

Declaration of competing interest

The authors declare that they have no known competing financial interests or personal relationships that could have appeared to influence the work reported in this paper.

Acknowledgements

This work has received funding from the Horizon Europe program, grant agreement number 101069789: project RELiEF – Recycling of Lithium from secondary raw materials and further. CENSE is supported by national funding through FCT – *Fundação para a Ciência e a Tecnologia*, I.P., in the scope of the projects UIDB/04085/2020 (DOI 10.54499/UIDB/04085/2020) and UIDP/04085/2020 (DOI 10.54499/UIDP/04085/2020). CHANGE is funded by FCT – *Fundação para a Ciência e a Tecnologia* under LA/P/0121/2020 (DOI 10.54499/LA/P/0121/2020). The authors would like to thank *Pegmatitica - Sociedade Mineira de Pegmatites, Lda,* for providing the working sample. This research was anchored by the RESOLUTION LAB, an infrastructure at NOVA School of Science and Technology.

Disclaimer: Funded by the European Union. Views and opinions expressed are however those of the authors only and do not necessarily reflect those of the European Union. Neither the European Union nor the granting authority can be held responsible for them.

Funded by the European Union

Data availability

No data was used for the research described in the article.

References

[1] S. Franzò, A. Nasca, The environmental impact of electric vehicles: a novel life cycle-based evaluation framework and its applications to multi-country scenarios,

J. Clean. Prod. 315 (2021) 128005, https://doi.org/10.1016/J.JCLEPRO.2021.128005.
[2] European Commission, "Fit for 55": council adopts key pieces of legislation delivering on 2030 climate targets, Brussels, Belgium, 2023.
[3] International Energy Agency, Technology and innovation pathways for zero-carbon-ready buildings by 2030, Paris, France, 2022.
[4] Y. Guo, S. Wu, Y.B. He, F. Kang, L. Chen, H. Li, Q.H. Yang, Solid-state lithium batteries: safety and prospects, EScience 2 (2022) 138–163, https://doi.org/10.1016/J.ESCI.2022.02.008.
[5] E.C. Evarts, Lithium batteries: to the limits of lithium, Nature 526 (2015) S93–S95, https://doi.org/10.1038/526s93a.
[6] D. Bradley, L.L. Stillings, B.W. Jaskula, L. Munk, A.D. McCauley, Lithium, professional paper 1802-K (2017) K1–K21. https://doi.org/10.3133/PP1802K.
[7] U.S. Geological Survey, 2021, Mineral commodity summaries 2021: U.S. Geological Survey, 200 p., https://doi.org/10.3133/mcs2021.
[8] U.S. Geological Survey, 2024, Mineral commodity summaries 2024: U.S. Geological Survey, 212 p., https://doi.org/10.3133/mcs2024.
[9] J. Speirs, M. Contestabile, Y. Houari, R. Gross, The future of lithium availability for electric vehicle batteries, Renewable Sustainable Energy Rev. 35 (2014) 183–193, https://doi.org/10.1016/J.RSER.2014.04.018.
[10] European Commission, RMIS - Battery supply chain challenges, (2023). https://rmis.jrc.ec.europa.eu/analysis-of-supply-chain-challenges-49b749 (accessed June 24, 2024).
[11] European Commission, Directorate-general for internal market industry entrepreneurship and SMEs, M. Grohol, C. Veeh, Study on the critical raw materials for the EU 2023 - Final report, 2023. https://data.europa.eu/doi/10.2873/725585 (accessed June 24, 2024).
[12] European Commission, Strategic autonomy: council gives its final approval on the critical raw materials act, (2024). https://www.consilium.europa.eu/en/press/press-releases/2024/03/18/strategic-autonomy-council-gives-its-final-approval-on-the-critical-raw-materials-act/(accessed March 27, 2024).
[13] S. Safari, B.G. Lottermoser, D.S. Alessi, Metal oxide sorbents for the sustainable recovery of lithium from unconventional resources, Appl. Mater. Today 19 (2020) 100638, https://doi.org/10.1016/J.APMT.2020.100638.
[14] G. Wei, Y. Liu, B. Jiao, N. Chang, M. Wu, G. Liu, X. Lin, X.F. Weng, J. Chen, L. Zhang, C. Zhu, G. Wang, P. Xu, J. Di, Q. Li, Direct recycling of spent Li-ion batteries: challenges and opportunities toward practical applications, iScience 26 (2023) 107676, https://doi.org/10.1016/J.ISCI.2023.107676.
[15] L. Wu, J. Zhang, Z. Huang, Y. Zhang, F. Xie, S. Zhang, H. Fan, Extraction of lithium as lithium phosphate from bauxite mine tailings via mixed acid leaching and chemical precipitation, Ore Geol. Rev. 160 (2023) 105621, https://doi.org/10.1016/J.OREGEOREV.2023.105621.
[16] C.M.G. Pires, A.B. Ribeiro, E.P. Mateus, H.A. Ponte, M.J.J.S. Ponte, Extraction of rare earth elements via electric field assisted mining applying deep eutectic solvents, Sustain. Chem. Pharm. 26 (2022) 100638, https://doi.org/10.1016/J.SCP.2022.100638.
[17] K. Islam, S. Murakami, Global-scale impact analysis of mine tailings dam failures: 1915–2020, Global Environ. Change 70 (2021) 102361, https://doi.org/10.1016/J.GLOENVCHA.2021.102361.
[18] X. Guo, J. Zhang, Q. Tian, Modeling the potential impact of future lithium recycling on lithium demand in China: a dynamic SFA approach, Renew. Sustain. Energy Rev. 137 (2021) 110461, https://doi.org/10.1016/J.RSER.2020.110461.
[19] P. Guedes, E.P. Mateus, J. Almeida, A. Ferreira, N. Couto, A.B. Ribeiro, Electrodialytic treatment of sewage sludge: current intensity influence on phosphorus recovery and organic contaminants removal, J. Chem. Eng. 306 (2016) 1058–1066, https://doi.org/10.1016/j.cej.2016.08.040.
[20] J. Almeida, C. Magro, A.R. Rosário, E.P. Mateus, A.B. Ribeiro, Electrodialytic treatment of secondary mining resources for raw materials extraction: reactor design assessment, Sci. Total. Environ. 752 (2020) 141822, https://doi.org/10.1016/j.scitotenv.2020.141822.
[21] A.B. Ribeiro, E.P. Mateus, L.M. Ottosen, G. Bech-Nielsen, Electrodialytic removal of Cu, Cr, and As from chromated copper arsenate-treated timber waste, Environ. Sci. Technol. 34 (2000) 784–788, https://doi.org/10.1021/es990442e.
[22] C.M.G. Pires, H.A. Ponte, M.T. Grassi, M.J.J.S. Ponte, A.B. Ribeiro, Extracting light rare earth elements by applying electric field assisted mining technique, Miner Eng 203 (2023) 108354, https://doi.org/10.1016/J.MINENG.2023.108354.
[23] P. Guedes, C. Magro, N. Couto, A. Mosca, E.P. Mateus, A.B. Ribeiro, Potential of the electrodialytic process for emerging organic contaminants remediation and phosphorus separation from sewage sludge, Electrochim. Acta 181 (2015) 109–117, https://doi.org/10.1016/j.electacta.2015.03.167.
[24] E. Velizarova, A.B. Ribeiro, L.M. Ottosen, A comparative study on Cu, Cr and As removal from CCA-treated wood waste by dialytic and electrodialytic processes, J. Hazard. Mater. 94 (2002) 147–160, https://doi.org/10.1016/S0304-3894(02)00063-8.
[25] Environmental Protection Agency, EPA method 3051A - Microwave assisted acid digestion of sediments, sludges, soils, and oils, 2007.
[26] Y. Huang, P. Li, R. Zhao, L. Zhao, J. Liu, S. Peng, X. Fu, X. Wang, R. Luo, R. Wang, Z. Zhang, Silica nanoparticles: biomedical applications and toxicity, Biomed. PharmacOther 151 (2022) 113053, https://doi.org/10.1016/J.BIOPHA.2022.113053.
[27] L. Gao, H. Wang, J. Li, M. Wang, Recovery of lithium from lepidolite by sulfuric acid and separation of Al/Li by nanofiltration, Minerals 10 (2020) 981, https://doi.org/10.3390/MIN10110981.
[28] M.A. Khater, Laser-induced breakdown spectroscopy for light elements detection in steel: state of the art, Spectrochim. Acta Part B At. Spectrosc. 81 (2013) 1–10, https://doi.org/10.1016/J.SAB.2012.12.010.
[29] P. Fichet, M. Tabarant, B. Salle, C. Gautier, Comparisons between LIBS and ICP/OES, Anal. Bioanal. Chem. 385 (2006) 338–344, https://doi.org/10.1007/S00216-006-0384-7.
[30] Y. Nie, J. Wang, J. Zhong, G. Li, Z. Wang, W. Peng, X. Li, R. Wang, G. Yan, H. Guo, Li+ attraction-repulsion synergy revealed by in-situ Raman spectroscopy for self-healing lithium metal anodes, Appl. Surf. Sci. 608 (2023) 155205, https://doi.org/10.1016/J.APSUSC.2022.155205.
[31] M. Vidal, A. Rigol, Sorption-desorption tests to characterize soils contaminated by heavy metals: implications for risk assessment, in: L. Simeonov, V. Sargsyan (Eds.), Soil Chemical Pollution, Risk Assessment, Remediation and Security. NATO Science for Peace and Security Series, Springer, Dordrecht, 2008, pp. 241–252, https://doi.org/10.1007/978-1-4020-8257-3_21.
[32] N. Yadav, S. Bhagat, S. Singh, Surface modification of metal oxide nanoparticles to realize biological applications, Encycl. Nanomater. 2 (2023) 450–477, https://doi.org/10.1016/B978-0-12-822425-0.00018-X.
[33] A. Chatterjee, J. Abraham, Desorption of heavy metals from metal loaded sorbents and e-wastes: a review, Biotechnol. Lett. 41 (2019) 319–333, https://doi.org/10.1007/S10529-019-02650-0/METRICS.
[34] J. Liu, R. Xu, W. Sun, L. Wang, Y. Zhang, Lithium extraction from lithium-bearing clay minerals by calcination-leaching method, Minerals 14 (2024) 248, https://doi.org/10.3390/MIN14030248, 2024, Vol. 14, Page 248.
[35] PubChem, Oxalic Acid, National Library of Medicine, 2024. https://pubchem.ncbi.nlm.nih.gov/compound/Oxalic-Acid. accessed January 18, 2024.
[36] PubChem, Citric Acid, National Library of Medicine, 2024. https://pubchem.ncbi.nlm.nih.gov/compound/Citric-Acid#section=Crystal-Structures. accessed January 18, 2024.
[37] Aqion, pH of organic acids and salts, (2024). https://www.aqion.de/site/ph-of-organic-acids (accessed September 26, 2024).
[38] K.V. Krishnamurty, G.M. Harris, The chemistry of the metal oxalato complexes, Chem. Rev. 61 (1961) 213–246, https://doi.org/10.1021/cr60211a001.
[39] G.M. Kirkelund, C. Magro, P. Guedes, P.E. Jensen, A.B. Ribeiro, L.M. Ottosen, Electrodialytic removal of heavy metals and chloride from municipal solid waste incineration fly ash and air pollution control residue in suspension - test of a new two compartment experimental cell, Electrochim. Acta 181 (2015) 73–81, https://doi.org/10.1016/j.electacta.2015.03.192.
[40] Y.B. Acar, A.N. Alshawabkeh, Principles of electrokinetic remediation, Environ. Sci. Technol. 27 (1993) 2638–2647, https://doi.org/10.1021/es00049a002.
[41] M. Van Der Hagen, J. Järnberg, Sulphuric, hydrochloric, Nitric and Phosphoric Acids, 140, University of Gothenburg, 2009.
[42] A. Król, K. Mizerna, M. Bożym, An assessment of pH-dependent release and mobility of heavy metals from metallurgical slag, J. Hazard. Mater. 384 (2020) 121502, https://doi.org/10.1016/j.jhazmat.2019.121502.
[43] C.D. Khedkar, S.D. Kalyankar, S.S. Deosarkar, Buffalo Milk, Encycl. Food Health (2016) 522–528, https://doi.org/10.1016/B978-0-12-384947-2.00093-3.
[44] J. Bardeen, Electrical conductivity of metals, J. Appl. Phys. 11 (1940) 88–111, https://doi.org/10.1063/1.1712751.
[45] C.T. O'Sullivan, Ohm's law and the definition of resistance, Phys. Educ. 15 (1980) 237, https://doi.org/10.1088/0031-9120/15/4/009.
[46] E. Velizarova, A.B. Ribeiro, E.P. Mateus, L.M. Ottosen, Effect of different extracting solutions on the electrodialytic remediation of CCA-treated wood waste Part I.: behaviour of Cu and Cr, J. Hazard. Mater. 107 (2004) 103–113, https://doi.org/10.1016/J.JHAZMAT.2003.09.011.
[47] A.J. García-Fernández, S. Espín, P. Gómez-Ramírez, E. Martínez-López, Oxalates, Encyclopedia of Toxicology: Third Edition, 2014, pp. 730–734, https://doi.org/10.1016/B978-0-12-386454-3.00526-1.
[48] P. Perumal, H. Niu, J. Kiventerä, P. Kinnunen, M. Illikainen, Upcycling of mechanically treated silicate mine tailings as alkali activated binders, Miner Eng 158 (2020) 106587, https://doi.org/10.1016/J.MINENG.2020.106587.
[49] C. Zheng, K. Jiang, Z. Cao, D.O. Northwood, K.E. Waters, H. Wang, S. Liu, K. Zhu, H. Ma, Agitation leaching behavior of copper–cobalt oxide ores from the Democratic Republic of the Congo, Minerals 13 (2023) 743, https://doi.org/10.3390/MIN13060743.
[50] L. Ji, H. Yu, Carbon dioxide sequestration by direct mineralization of fly ash, in: Fernando Pacheco-Torgal, Caijun Shi, Angel Palomo Sanchez (Eds.), Woodhead Publishing Series in Civil and Structural Engineering, Carbon Dioxide Sequestration in Cementitious Construction Materials, Woodhead Publishing, 2018, pp. 13–37, https://doi.org/10.1016/B978-0-08-102444-7.00002-2.
[51] A.Y. Fosu, N. Kanari, D. Bartier, H. Hodge, J. Vaughan, A. Chagnes, Physico-chemical characteristics of spodumene concentrate and its thermal transformations, Materials. (Basel) 14 (2021) 7423, https://doi.org/10.3390/MA14237423/S1.
[52] C. Amador, L. Martin de Juan, Strategies for structured particulate systems design, Comput. Aided Chem. Eng. 39 (2016) 509–579, https://doi.org/10.1016/B978-0-444-63683-6.00019-8.
[53] Y. Zhang, J. Zhang, L. Wu, L. Tan, F. Xie, J. Cheng, Extraction of lithium and aluminium from bauxite mine tailings by mixed acid treatment without roasting, J. Hazard. Mater. 404 (2021) 124044, https://doi.org/10.1016/J.JHAZMAT.2020.124044.
[54] A.B. Ribeiro, J.M. Rodríguez-Maroto, Electroremediation of heavy metal-contaminated soils - processes and applications, in: M.N.V. Prasad, K.S. Sajwan, R. Naidu (Eds.), Trace Elements in the Environment: Biogeochemistry, Biotechnology, and Bioremediation, Taylor & F, CRC Press, Florida, USA, 2006, pp. 341–368, https://doi.org/10.1385/BTER:109:3:301.
[55] T. Aaltonen, O. Nilsen, A. Magrasó, H. Fjellvåg, Atomic layer deposition of Li_2O-Al_2O_3 thin films, Chem. Mater. 23 (2011) 4669–4675, https://doi.org/10.1021/cm200899k.

[56] S.J. Visco, E. Nimon, L.C. De Jonghe, Secondary batteries – metal-air systems | lithium–air, Encycl. Electrochem. Power Sources (2009) 376–383, https://doi.org/10.1016/B978-044452745-5.00184-2.
[57] X. Zeng, J. Li, B. Shen, Novel approach to recover cobalt and lithium from spent lithium-ion battery using oxalic acid, J. Hazard. Mater. 295 (2015) 112–118, https://doi.org/10.1016/J.JHAZMAT.2015.02.064.
[58] Y. Wen, X. He, S. Di, K. Liu, D. Li, J. Du, Comparative of malonic acid aqueous solution and malonic acid-based deep eutectic solvent for LiCoO2 cathode materials recovery: leaching efficiency and mechanism, J. Environ. Chem. Eng. 11 (2023) 110979, https://doi.org/10.1016/J.JECE.2023.110979.
[59] H. Strathmann, Chapter 6 Electrodialysis and related processes, in: Richard D. Noble, S.Alexander Stern (Eds.), Membrane Science and Technology, Elsevier, 1995, pp. 213–281, https://doi.org/10.1016/S0927-5193(06)80008-2, 2.
[60] E. Mroczek, G. Dedual, D. Graham, L. Bacon, Lithium extraction from Wairakei Geothermal fluid using electrodialysis, in: Proceedings World Geothermal Congress, Melbourne, Australia, 2015, pp. 19–25, 19-25 April 2015, https://www.geothermal-energy.org/pdf/IGAstandard/WGC/2015/39000.pdf?.
[61] S.K. Sarker, N. Haque, M. Bhuiyan, W. Bruckard, B.K. Pramanik, Recovery of strategically important critical minerals from mine tailings, J. Environ. Chem. Eng. 10 (2022) 107622, https://doi.org/10.1016/J.JECE.2022.107622.